[American Journal of Science, Vol. 262, January 1964, P. 26-55]

EXPERIMENTAL DEFORMATION OF QUARTZ SINGLE CRYSTALS AT 27 TO 30 KILOBARS CONFINING PRESSURE AND 24°C*

J. M. CHRISTIE, H. C. HEARD,** and P. N. LaMORI†

Department of Geology and Institute of Geophysics, University of California, Los Angeles 24, California

ABSTRACT. Oriented cylindrical samples cored from clear untwinned quartz crystals were deformed in compression in a piston and cylinder device, using bismuth as the pressure medium. Manv samples were deformed to failure in the BiII⇄BiIII transition at 27 kb and the ultimate strengths of these samples are recorded; the values show a high degree of consistency. Strengths of samples compressed parallel to the *c*-axis are significantly higher than those of crystals compressed in other directions.

The samples failed by rupture along "faults" in planes of high shear stress. These are crystallographically controlled: they are commonly parallel to the basal plane *c* and the unit rhombohedra *r* and *z*, and rarely to the prisms *m* and *a*. The main faults are generally inclined at less than 45° to the axis of compression but in crystals of two orientations they are inclined at angles greater than 45° to the compression axis. The faulting is apparently a fracture phenomenon. Thin zones of isotropic material, with lower refractive index than quartz, are present along many faults; some of these zones contain minute amounts of crystalline material, with higher indices and lower birefringence than quartz, probably coesite. The origin of these new phases is discussed.

Faulting takes place at lower shear stress on the base than on the unit rhombohedra, and on the unit rhombohedra than on the prism planes. Shear strengths along different planes are unrelated either to the bond density across these planes, the shear moduli, or the theoretical strengths. Other workers have shown that at higher temperatures quartz deforms by slip on the base and other planes including rhombohedral planes and possibly prism planes; the critical shear stresses for slip on the different planes, insofar as they are known, appear to vary in the same way as those for faulting. It is suggested that faulting is initiated by small amounts of slip on the planes; this gives rise to submicroscopic cracks which become large enough to propagate as brittle fractures.

INTRODUCTION

At the time when this study was begun, there was no unequivocal evidence that plastic deformation of quartz had been produced experimentally in the laboratory. It has been shown by many workers that high confining pressure tends to inhibit the fracture of materials and thus enhances the possibility of plastic flow taking place. In view of this, the present series of experiments was undertaken to determine if quartz would yield by plastic deformation at confining pressures in the region of 25 to 30 kilobars (kb) at room temperature, and, if so, to identify the mechanisms of deformation.

The experiments were carried out in a piston and cylinder apparatus, designed by G. C. Kennedy (Kennedy and LaMori, 1961). Cylinders cored from single crystals of quartz were deformed in compression, using bismuth as the pressure medium. The dimensions of the sample and the assembly were arranged so that the quartz would be deformed as the bismuth underwent a polymorphic transition at 27 kb, thus fixing the confining pressure.

* Publication No. 237, Institute of Geophysics and Planetary Physics, University of California, Los Angeles, California.

** Present address: Shell Development Co., Exploration and Development Research Division, Houston 25, Texas.

† Present address: The Technological Institute, Department of Materials Science, Northwestern University, Evanston, Illinois.

In all the experiments the quartz failed by sudden rupture as it does at lower confining pressures. An examination of thin sections of the deformed samples showed that the quartz had deformed by shear, or faulting, along rational crystallographic planes. One of the main objectives of the study is the examination of the mechanism by which this faulting takes place. The experiments were extended to a number of different orientations to provide a comparison of the strengths in different crystallographic directions and to determine which crystallographic planes are the fault-planes in specimens of different orientations.

EXPERIMENTAL METHODS AND PROCEDURE

Apparatus and Experimental Procedure.—The equipment used to deform the samples is a piston and cylinder device (Kennedy and LaMori, 1961) similar to those of Coes (1955), Hall (1958), and Boyd and England (1960a). It consists of a cylindrical tungsten carbide pressure vessel (G. E. Grade 883) supported by hardened steel (S.A.E. 4340) binding rings as shown in figure 1. The steel binding rings are pressed together with 1 percent interference on a taper with a 3° included angle. The ends of the carbide pressure vessel are supported by compression between large hydraulically-driven platens through which the carbide piston passes into the pressure vessel. The piston fits the cylinder within 0.0002 inch.

The principle employed in the experiments was as follows. At room temperature bismuth undergoes two polymorphic transitions between 25 and 30 kb, BiI $\rightleftarrows$ BiII at 25.4 kb and BiII $\rightleftarrows$ BiIII at 27.0 kb (Kennedy and LaMori, 1962). There is a considerable change of volume (approximately 8 percent) in the range of these transitions. Thus if the pressure vessel is filled with bismuth and then compressed, there is a large piston displacement with relatively slight change of pressure within the bismuth. The sample assembly in the experiments (fig. 1) was designed so that the deformation of the quartz would take place entirely within the pressure range of the transitions. The quartz cylinder and a tungsten carbide endpiece were sealed within a machined copper jacket which

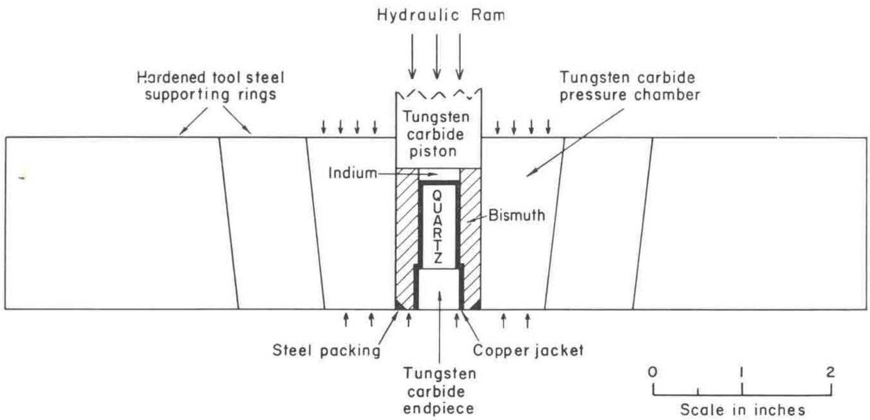

Fig. 1. Section through the apparatus and sample assembly. Scale is approximately correct for runs with the larger crystals.

was fitted into a hole machined in a previously-compacted slug of bismuth. The disc of indium between the quartz sample and the piston acts as a space-filler; indium was used because of its very low strength. It ensures that the quartz is compressed hydrostatically in the early stages of the experiment. During the experiment, as the loading piston is advanced, the indium is progressively squeezed aside along the piston face and between the bismuth and the copper jacket, until at a certain piston displacement, which depends on the geometry of the assembly, the compressibility of the bismuth and indium, and the elastic constants of the quartz, the quartz is in contact with the piston. The quartz is then compressed axially by the piston, at a confining pressure equal to that of the bismuth. The sample assembly was designed so that the piston would contact the quartz within the first transition (BiI $\rightleftarrows$ BiII) and the quartz fail before the completion of the second transition (BiII $\rightleftarrows$ BiIII).

In the first experiments quartz cylinders 1.0 cm in diameter and 2.5 cm long were deformed in a pressure vessel 2.5 cm in diameter. The records in these experiments showed that a large proportion of the cylinders failed after the second transition was complete. It is estimated that the confining pressure at the time of failure in these experiments was between 27 and 30 kb. It was impossible to calculate the strengths accurately for these experiments. The assembly was redesigned to ensure that the deformation would be complete (to failure) within the range of the second bismuth transition. This involved the use of smaller quartz samples (0.45 cm diameter, 1.3 cm long), thinner copper jackets, and a larger volume of bismuth, relative to the quartz. These were deformed in a cylinder of smaller diameter (1.27 cm). All the strength determinations reported below are for samples that failed during the second transition of the bismuth, when the confining pressure was 27 kb.

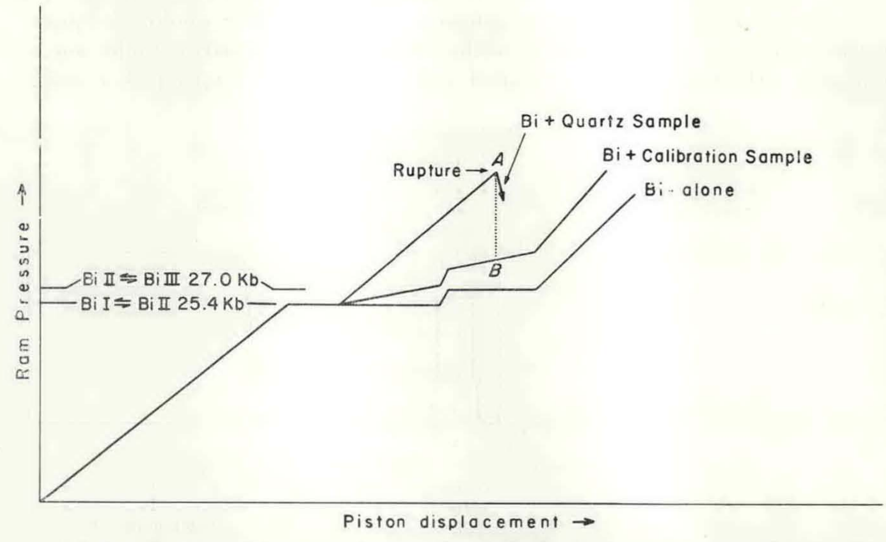

Fig. 2. Diagrammatic representation of records showing ram pressure and piston displacement.

The data were automatically plotted by an X-Y recorder, with the ram pressure along one axis and the displacement of the piston along the other (fig. 2). The bismuth transitions are indicated by a large piston displacement with little change in pressure. When the quartz made contact with the piston the ram pressure increased much more rapidly than in the normal transition in a sample containing only bismuth (fig. 2). In most of the experiments the quartz failed with a loud report, and the records show a rapid decrease of pressure and increase of piston displacement at the time of failure. After rupture, the sample was unloaded, rapidly in some experiments and slowly in others. In three experiments, the sample was unloaded when the axial load was just below the rupture point, as determined in earlier experiments. These samples were sectioned as the others were (see below) for comparison with the ruptured samples.

Because of high (and undetermined) friction between the piston and packings and the pressure vessel in the experiments, and the small but finite strengths of the bismuth and copper in the assembly, the strengths of the samples were not computed directly from the curves. Instead, calibration runs were made using samples of exactly the same geometry as those for quartz experiments, but in which the quartz cylinder was replaced by one of a material with low strength. Indium was chosen as its strength at these pressures (approximately 0.5 kb) is negligible compared with that of quartz and its compressibility is almost identical with that of quartz. In the idealized curves in figure 2, the vertical distance (AB) between the rupture point (A) for a quartz sample and the point (B) on the curve for the calibration run is proportional to the strength of the quartz, minus the load supported by a similar sample of indium under the same conditions. The axial stress on the quartz can be computed from the ram pressure, since the cross-sectional area of the ram and the initial cross-sectional area of the quartz cylinder are known. The accuracy of the Heise-Bourdon gauge used to measure the pressure behind the ram is stated

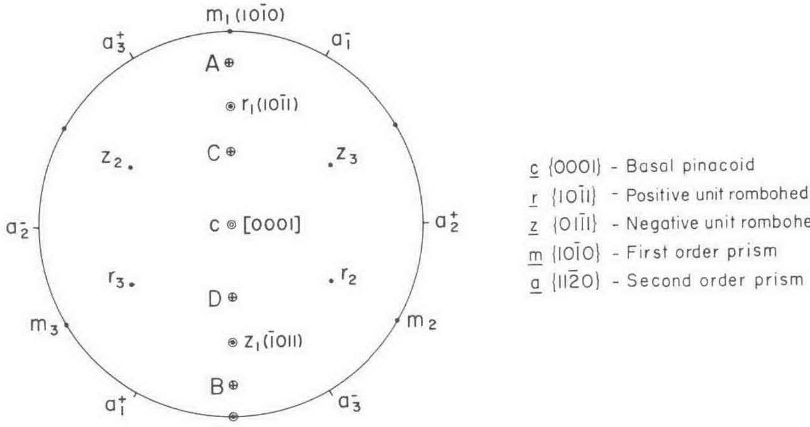

Fig. 3. Equal-area projection (lower hemisphere) showing the common crystal planes of quartz and the convention regarding polarity of the *a*-axes. Directions in which samples were cored are represented by circles.

to be ± 0.5 bars. In converting the ram pressure to axial load on the quartz cylinder, this is equivalent to approximately ± 0.5 kb axial stress on the quartz; this is therefore the precision with which the measurements were made. Since the correction for the strength of indium was approximately the same as the estimated precision of the measurements, no correction was made for this. Changes in the cross-sectional area of the quartz sample due to (1) compressibility of the quartz and (2) elastic distortion of the sample under load are of opposite sign and cancel each other within the precision of the measurements.

The average strain-rate in the quartz during loading was 3×10^{-4} per second. The samples that were deformed but not ruptured showed no macroscopic evidence of deformation. Thus most of the permanent strain in the other samples must have been produced almost instantaneously at rupture, and the deformation before rupture was therefore predominantly elastic.

Preparation of samples and thin sections.—The deformed samples were to be examined optically in thin section, and since it is impossible to determine the orientation of the *a*-axes optically, it was necessary to devise a method of coring and marking the samples so that the orientation of the cylinders, and ultimately the thin sections, would be fully known.

The cylinders were cored from large optical-quality quartz crystals using a diamond-impregnated coring drill. Large crystals with well-developed prism and rhombohedral faces were etched lightly with 40 percent hydrofluoric acid. The shapes of the etch-pits on these faces were used (Ichikawa, 1915) to dis-

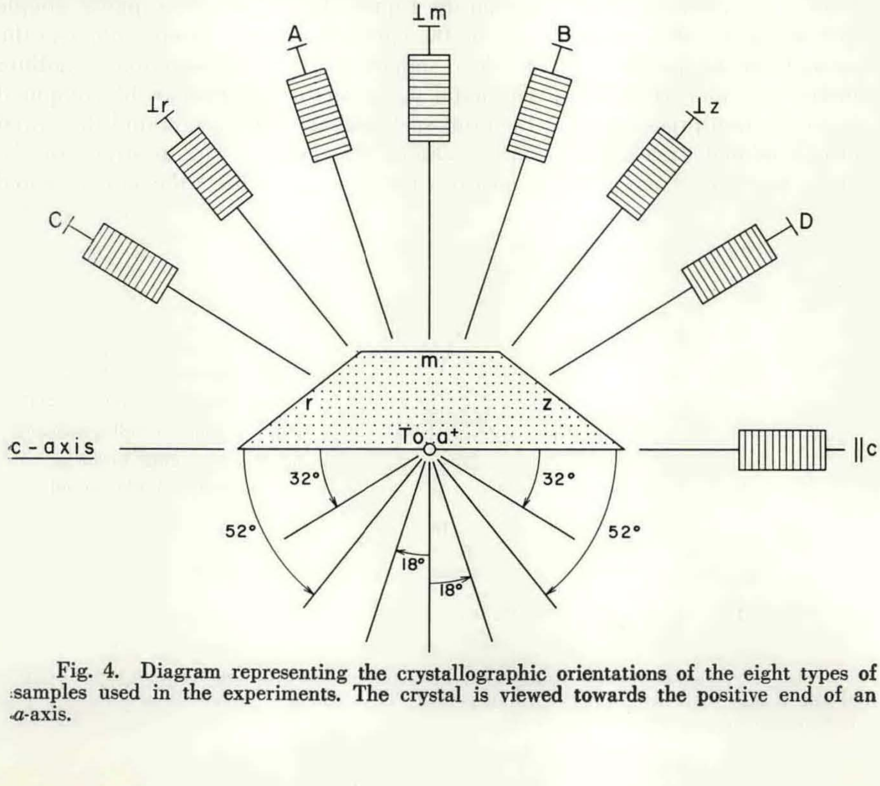

Fig. 4. Diagram representing the crystallographic orientations of the eight types of samples used in the experiments. The crystal is viewed towards the positive end of an *a*-axis.

tinguish the positive and negative unit rhombohedra, r {10$\bar{1}$1} and z {01$\bar{1}$1} respectively, and also to detect the presence of twinning (on the Dauphiné or Brazil laws) at the surface of the crystals. Twinned crystals were rejected. The etch-pits revealed the "hand" of the crystals and the orientation and polarity of the a-axes. The cylinders were marked in such a way that their orientations were fully known from the markings.

Eight orientations of cylinders, designated $\|c$, $\perp r$, $\perp z$, $\perp m$, A, B, C, and D (fig. 3), were used. The axes of all the cylinders lie in a plane normal to one of the a-axes; they are inclined to the c-axis at the angles shown in figure 4. One end of each cylinder was marked with an arrow parallel to an a-axis and pointing to the positive end of this a-axis. Another arrow inscribed on the cylindrical surface, parallel to the cylinder axis, in a position corresponding to the point of the arrow on the end of the cylinder (see fig. 5); the longitudinal arrow was marked with the direction of the cylinder (c, r, z, m, A, B, C, or D) and a^+ to indicate that the positive end of the a-axis emerges on this side of the cylinder. This convention has the advantage that all the cylinders carry analogous but distinctive markings, and the orientation of a cylinder is known if the marking on either the end or the side of the cylinder survives the experiment.

After deformation the jacketed samples were removed from the bismuth. They generally retained their cohesion, though planes with displacements were visible in the copper jacket (pl. 1A). The jackets were perforated or partially removed, and the samples were impregnated with and embedded in a clear thermo-setting plastic to prevent disintegration during the preparation of thin sections. The sections were prepared, with one of two orientations (see below) from each of the deformed cylinders.

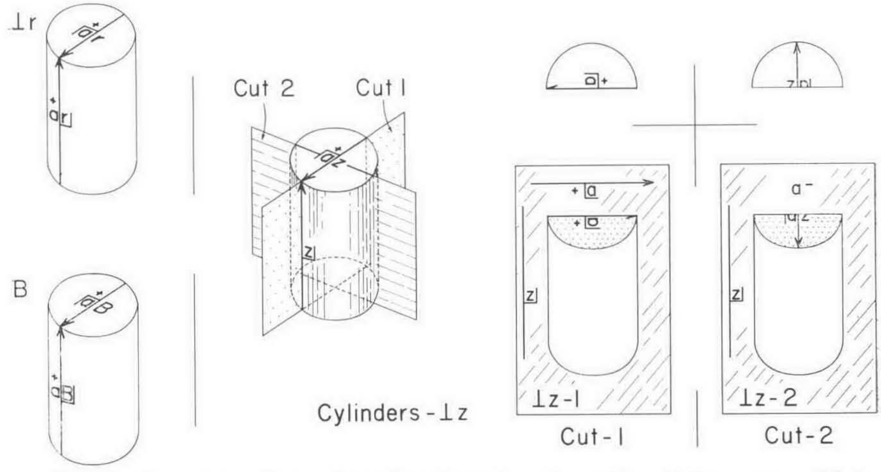

Fig. 5. Conventions for marking the orientation of crystals and thin sections. Marks on cylinders $\perp r$ and B are shown on the left. On the right are the two types of thin section cut from a $\perp z$ cylinder and the stages in the preparation and marking of the thin section: top, half of the cylinder ground away; bottom, the half-cylinder mounted on marked slide ready for grinding and finishing.

The convention for sectioning and marking the orientation on the thin sections (fig. 5) is the same for cylinders of all orientations. The two orientations of thin sections are designated *1-cut* (parallel to the cylinder axis and parallel to the *a*-axis arrow) and *2-cut* (parallel to the axis of the cylinder and perpendicular to the *a*-axis arrow). The selection of section-plane for any specimen depended on the orientation of the planes of displacement visible on the copper jacket; the specimens were sectioned so that the main shear-planes would be almost perpendicular to the section. Half of the cylinder and plastic mount were ground away in the manner illustrated (fig. 5), and the half-cylinder was cemented to a slide as shown. Care was taken that in all 1-cut sections the slide would be viewed on the microscope stage with the positive end of the *a*-axis distinguished (to the right) and in all 2-cut sections, the slide would be viewed from the positive to the negative end of the *a*-axis. By following this convention it is possible to index any planar structures of rational orientation present in the deformed samples (subject to small errors inherent in the sectioning operations, which may be determined in part and are discussed below).

Petrographic examination of the samples.—The thin sections were placed on a four-axis universal stage on a polarizing microscope, and the structures in them were examined in detail in transmitted light. Since one of the objectives of the study was to try to reproduce the structures found in naturally deformed rocks, such as undulatory extinction and deformation lamellae, a very careful search was made for these features.

EXPERIMENTAL RESULTS

The ultimate strengths of the quartz cylinders were determined, by the method outlined above, for all the samples in which the records showed clearly that the deformation began and proceeded to rupture within the range of the two bismuth transitions. These are listed in table 1. The confining pressure is represented as the least principal stress (σ_3), and the total axial stress on the sample as the maximum principal stress (σ_1). This convention, in which a compressive stress is considered positive, is that usually used by geologists.

The larger samples used in the first experiments showed considerable variation in the axial stress at rupture, but reduction of the data showed that most of these had failed at confining pressures above 27 kb. The strengths of the smaller cylinders, all of which failed in the BiII $\rightleftarrows$ BiIII transition at 27 kb, showed much better reproducibility. For this reason rupture strengths are reported only for the second group of samples. Petrographic studies have been

---

PLATE 1

A. Components of equipment and sample assembly. In front of the pressure vessel are, left to right, the piston, two deformed samples in copper jackets, an undeformed sample, carbide endpiece, copper jacket, bismuth slug, and steel packing.

B. Thin section of a large crystal compressed normal to *z* (759), showing development of main fault parallel to the base and subsidiary sets of rhombohedral faults (*r*). Plane-polarized light.

C. Thin section of a large crystal compressed parallel to B (765), showing two sets of rhombohedral (*r*) faults more or less equally developed. Between crossed polarizers.

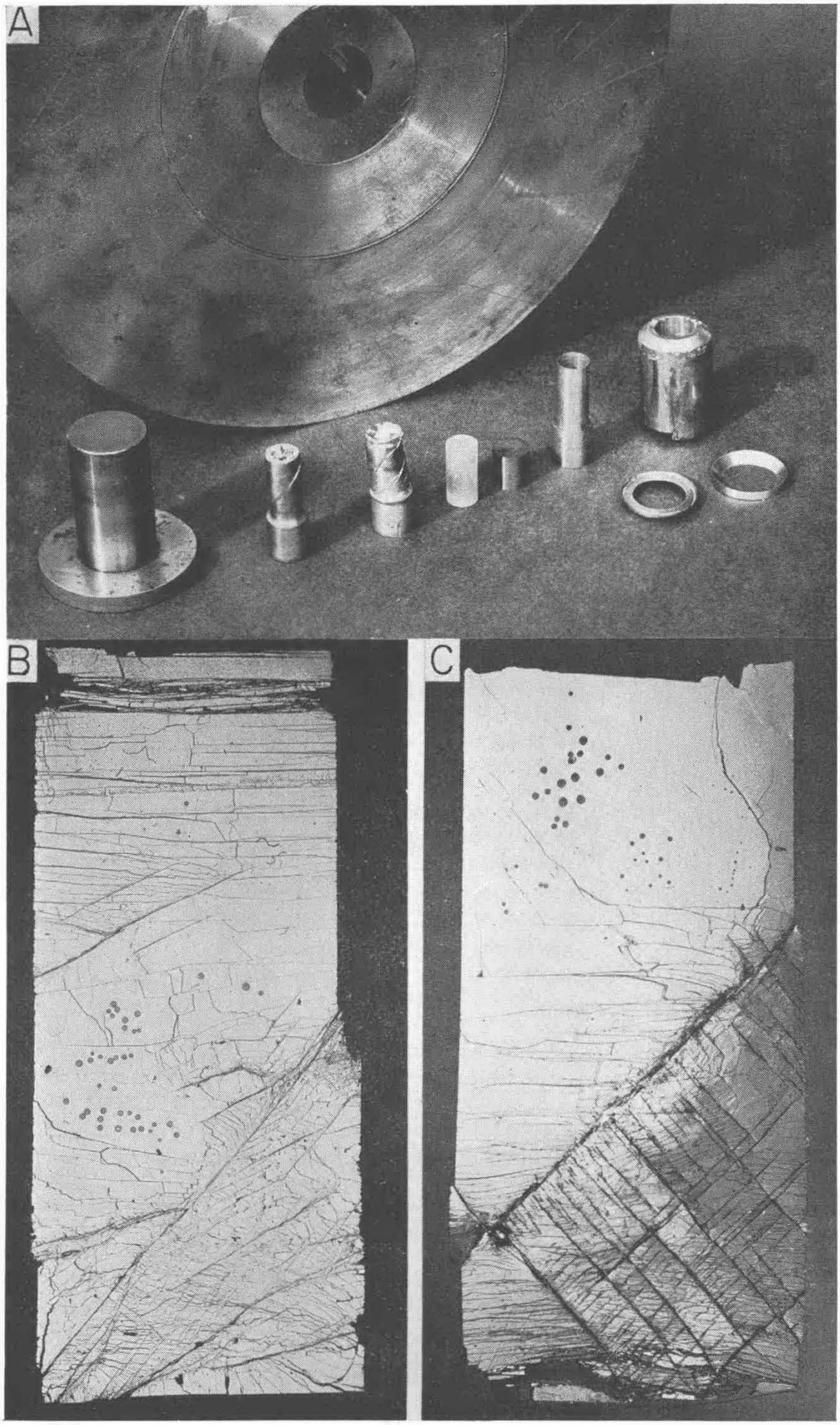
A
B
C

TABLE 1

Orientation of cylinders	Experiment number	Strength of specimens $(\sigma_1\text{-}\sigma_3)$ in kilobars		Stresses in main fault at rupture in kilobars	
				τ	σ
$\|\|$c	781	46.7		22.6	44.7
$\|\|$c	782	45.4	Average = *46.5*	22.0	44.2
$\|\|$c	783	47.3		22.9	44.9
$\perp$r	785	42.1		20.4	43.0
$\perp$r	786	41.6	Average = *42.6*	20.2	42.8
$\perp$r	787	44.2		21.4	43.8
$\perp$z	780	40.8	Average = *42.1*	19.8	42.5
$\perp$z	789	43.4		21.0	43.5
$\perp$m	779	41.0	Average = *42.8*	14.7	33.3
$\perp$m	790	44.6		16.0	33.8
B	792	46.2	Average = *44.3*	23.0	48.5
B	793	42.3		21.1	46.8
A, C, D		Not determined			

made of sections prepared from both groups of samples, and the structures in the samples from both groups are identical for any given orientation (table 2).

The strengths obtained from the smaller samples (table 1) show very good reproducibility compared with those obtained in earlier studies of the strength of quartz at room temperature (summarized in Griggs, Turner, and Heard, 1960). The mean deviations of the measurements range from 0.7 kb, for cylinders parallel to the *c*-axis, to 2.0 kb for cylinders compressed parallel to *B*. The values for the cylinders compressed parallel to the *c*-axis are consistently higher than those for the other orientations; the values for the other orientations are more variable and show considerable overlap in their range. For this reason experiments with smaller samples were not carried out for all the eight orientations, as an unreasonable number of runs would have been necessary to demonstrate a relationship between the strength and crystallographic orientation of the cylinders.

PETROGRAPHIC OBSERVATIONS

Structures in the deformed quartz.—The most marked characteristic of all the section, except those not deformed to rupture, is the presence of many fractures with different orientations. The most obvious features in the thin sections are thin, well-defined zones of shearing, along which there are generally marked displacements of the crystal. The structures fall within the category referred to by Griggs and Handin (1960, p. 348) as "faults",[1] and this term is adopted for these features. The displacements on these faults account for most of the permanent strain in the crystals. The faults commonly occur in parallel sets in a specimen, and many specimens contain two or more sets (pl. 1B, C). It is generally possible to identify one *main* fault, or set of faults, along which most of the displacement has occurred and against which subsidiary faults are terminated (pl. 1B). But this distinction is not always possible: in some samples two

[1] A "fault" is defined as "a localized offset parallel to a more or less plane surface of nonvanishing shear stress" (Griggs and Handin, 1960).

TABLE 2

Orientation of cylinders	Experiment number	Orientations of faults
$\|\|c$	753	r_1, r_2, z_1, z_2, z_3
$\|\|c$	755	$r_1, r_2, r_3, z_1, z_2, z_3$
$\|\|c$	781	$z_1, r_2, z_3, r_3, r_1, z_3$
$\|\|c$	782	z_1, z_2, r_2, (0001)
$\perp r$	749	**(0001)**, z_2, z_3
$\perp r$	750	**(0001)**, z_2, z_3
$\perp r$	761	**(0001)**, z_2, z_3, r_1, r_2
$\perp r$	785	**(0001)**, z_2, z_3
$\perp r$	786	**(0001)**, z_2, z_3
$\perp r$	787	**(0001)**, z_2, z_3
$\perp z$	754	**(0001)** —
$\perp z$	759	**(0001)**, r_2, r_3, m_1
$\perp m$	756	$\mathbf{r_3}, \mathbf{z_3}, z_1, z_2, r_2$
$\perp m$	758	$\mathbf{r_2}, \mathbf{z_2}, z_1, z_2, r_1, r_2$
$\perp m$	784	z_1, r_2, r_3
$\perp m$	788	z_2, r_2, z_3, z_1, (0001)
$\perp m$	790	r_1, r_2, z_2, z_3, (0001)
A	762	$\mathbf{z_3}, z_2, r_1, r_3, m_1, m_3$
A	763	$\mathbf{z_3}, z_2, r_1$
A	791	z_3, z_2, (0001), m_1
B	765	$\mathbf{r_3}, r_2, z_1$
B	770	$\mathbf{r_2}, r_3, z_1$
B	791	r_2, r_3, z_2, m_3, (0001)
B	793	r_2, r_3
C	760	$\mathbf{z_2}$, (0001), z_3
C	766	$\mathbf{z_2}$, (0001), z_3
C	767	$\mathbf{z_3}$, (0001), z_2, a_3
D	768	r_3, (0001), r_2
D	769	r_1, r_2, r_3, (0001)

or more sets are more or less equally developed (pls. 1C, 2B), and in others two non-parallel sets of faults are present in a broad fault-zone.

Associated with some of the faults are closely-spaced sets of fractures showing no displacements (pl. 2A). These resemble the so-called "feather-fractures" or "feather-joints" (Billings, 1954, p. 117) along some geological faults, and we shall refer to them by the former name. Feather-fractures are generally considered to be extension fractures originating with, or immediately after, the fault.

In addition to these two types of planar structures, there are other regular sets of fractures which show no displacements parallel to their surfaces; the best-developed set is generally parallel to the ends of the cylinders (pl. 1B). There is evidence that these are extension fractures produced on unloading the samples. Some long curved cracks are also present in the material (pl. 1B).

At small distances from the faults the quartz commonly shows little evidence of penetrative strain and may be indistinguishable from the undeformed material used in the experiments. Locally in some of the samples, however, there are extremely fine structures which can be recognized between crossed polarizers when the crystal is at extinction; these are described in more detail below. In the immediate vicinity of the faults, on the other hand, there is a narrow zone in which the optical orientation differs from that of the host crystal (pl. 2C). There is considerable fracturing on a very fine scale in these zones of reoriented material, and it is possible that the disorientation has resulted from rotation of submicroscopic blocks bounded by fractures. Along the faults themselves a thin zone of brownish, optically isotropic material may be present. In many instances this isotropic material contains tiny particles of fragmented quartz. Minute crystals of an optically anisotropic material of high refractive indices have also been observed in fault-zones in a few crystals.

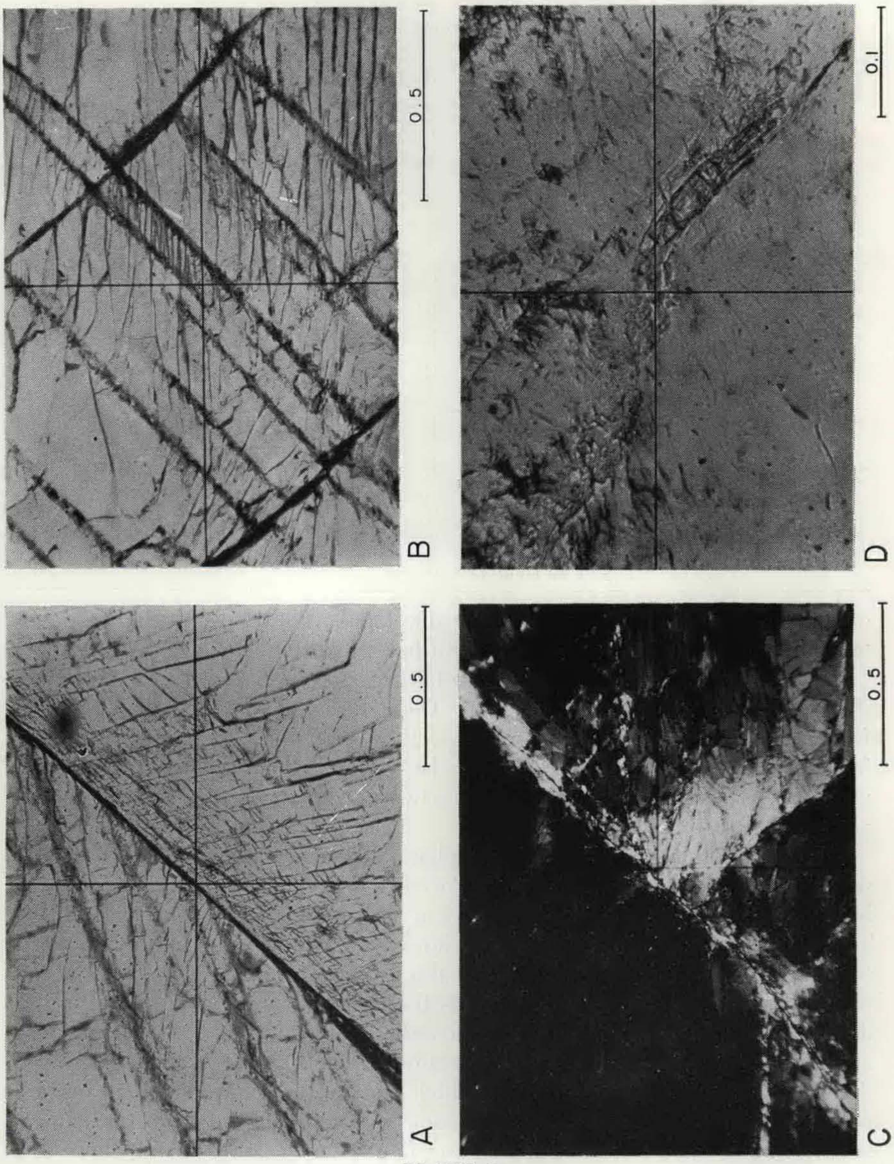

PLATE 2

Photomicrographs of structures and a new crystalline phase in thin sections of deformed crystals. Scales are in mm.

A. A fault with feather-fractures (lower right) and a subsidiary set of faults (upper left), inclined to the thin section, terminating against it. Direction of compression north-south. Plane-polarized light.

B. Intersecting sets of faults. Plane-polarized light.

C. Reoriented material along faults, between crossed polarizers. Note intense fracturing in reoriented quartz.

D. Segment of a thick fault-zone containing an elongate aggregate of slightly birefringent crystalline material with high indices (probably coesite). Plane-polarized light.

In the examination of the deformed crystals, a careful search was made for undulatory extinction and deformation lamellae of the type found in naturally deformed quartz. Both of these features were observed only in a small part of one sample (766) ; the lamellae were approximately basal and associated with slight undulatory extinction in zones parallel to the *c*-axis of the crystal.[2] In this experiment the piston broke, and there was consequently very rapid unloading of the sample. The stress conditions in the experiment were unknown, and it was impossible to determine whether the structures formed during loading or unloading. Similar structures were not produced in other samples of the same orientation. Though this is probably the first case in which these structures were definitely produced experimentally, it is relatively insignificant, since the conditions at formation were unknown. These structures have now been produced extensively in single crystals and aggregates (Carter, Christie, and Griggs, 1961; Christie, Carter, and Griggs, 1961) at similar confining pressures and higher temperatures. Heard (ms) has also produced these structures in quartzite at more moderate pressures and temperatures (5 kb and 300 to 500°C) in experiments at slow strain rates (10^{-6} to 10^{-8}/sec).

Orientation of the Planar Structures.—The orientations of the planar structures were measured in equally spaced traverses across the crystals parallel to the ends of the cylinders. It should be noted that a single planar structure extending diagonally across a section might be measured and recorded several times. The orientation of the *c*-axis was also determined in different parts of each section.

All planar features, including faults, feather-fractures, and other planar and curved fractures, were measured in several sections; in the majority of the crystals, however, the orientations of only the faults, feather fractures, and the optic axis were measured. Measurements were made on nearly planar portions of the curved fractures in those sections in which they were examined. Since it is impossible to reproduce the orientation data for all the specimens, only representative diagrams are reproduced. Data for the remaining samples are summarized in tabular form (table 2). Orientations are shown on an equal-area projection, using the lower hemisphere; the primitive circle in each projection represents the plane of the thin section in which the structures were measured.

The attitudes of the different types of structures in two specimens, 749 and 759 are shown in figures 6 and 7 respectively. A strong preferred orientation of all the structures is evident in the diagrams.

Specimen 749 (fig. 6) was cored and compressed perpendicular to the plane r_1. The most prominent set of faults is parallel to the base, and other well-developed faults are parallel to the negative unit rhombohedra z_2 and z_3. The feather-fractures, which are all associated with the basal faults, are approximately parallel to z_1, though there is a greater spread of orientation than for the faults; this parallelism of the fractures with z_1 may be fortuitous, since these structures are probably extension fractures, controlled by the orientation of the stress in the vicinity of the fault immediately after failure. The best-

[2] It is not possible to photograph these structures satisfactorily as they are visible only when the section is tilted steeply on the U-stage.

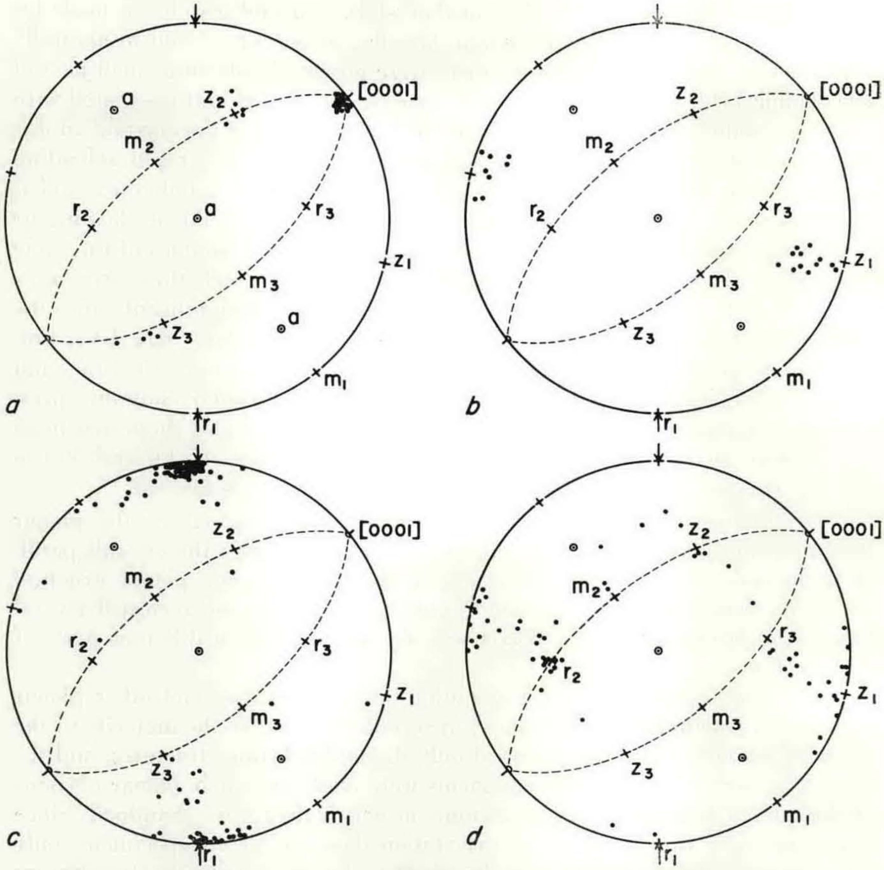

Fig. 6. Orientation of planar structures in specimen 749. The primitive circle in the equal-area projections is the plane of the thin section and the orientation of the crystal axes and poles of rhombohedral and prism planes are shown. (*a*) Poles of faults. (*b*) Poles of feather-fractures. (*c*) Poles of other prominent planar fractures. (*d*) Poles of planar portions of curved fractures.

developed set of planar fractures is perpendicular to the cylinder axis (that is, parallel to r_1), but there are also fractures sub-parallel to other rhombohedral and prism planes. The planar portions of curved fractures also show a tendency to be controlled by the unit rhombohedral planes (r, z) and to a lesser extent, the prism planes (m).

In specimen 759 (fig. 7), cored and compressed normal to z_1, the most prominent set of faults is also parallel to the base, and faults parallel to r_2 and r_3 and the prism m_1 are also present. Feather-fractures are associated with the basal faults and show a tendency to be parallel to r_1 (which may again be fortuitous); a few, possibly formed along the same faults on unloading, are almost parallel to z_1. The other fractures, not separated for this specimen, show a very weak preferred orientation; there are weak concentrations parallel to some of the rhombohedral planes.

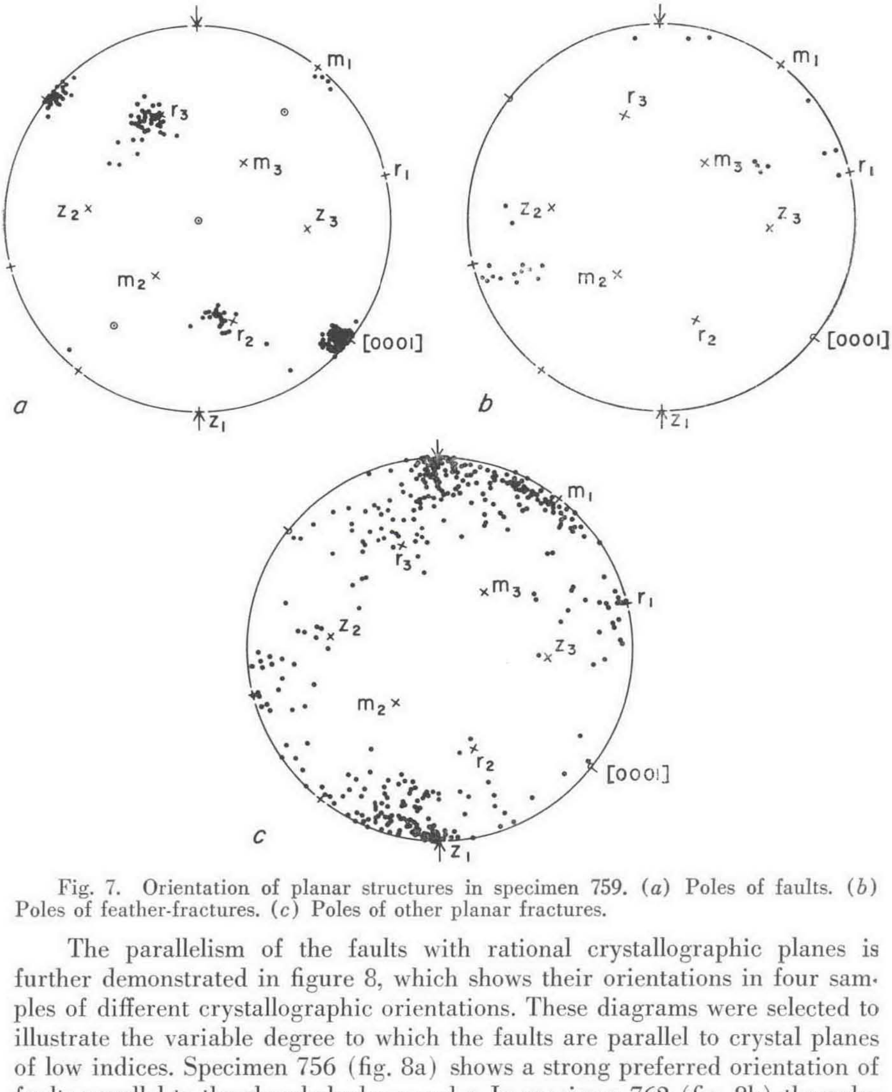

Fig. 7. Orientation of planar structures in specimen 759. (*a*) Poles of faults. (*b*) Poles of feather-fractures. (*c*) Poles of other planar fractures.

The parallelism of the faults with rational crystallographic planes is further demonstrated in figure 8, which shows their orientations in four samples of different crystallographic orientations. These diagrams were selected to illustrate the variable degree to which the faults are parallel to crystal planes of low indices. Specimen 756 (fig. 8a) shows a strong preferred orientation of faults parallel to the rhombohedra r and z. In specimen 762 (fig. 8b) the poles of the faults spread along great-circles (r_3-m_3-z_3; r_2-m_2-z_2) corresponding to important zones in the crystal; this suggests that some of the fault surfaces, if seen at greater magnification, might be step-like combinations of two planes with low indices (for example, z_3 and r_3). In figure 8c (specimen 765) the concentrations of poles of the measured faults lie slightly away from the points representing the r and z planes. However, the angles between the measured planes correspond to the interfacial angles between the rhombohedral planes r_2 and r_3. Moreover, the measured c-axis is inclined to the predicted c-axis by approximately 10°, and it is evident that a rotation of the measured planes

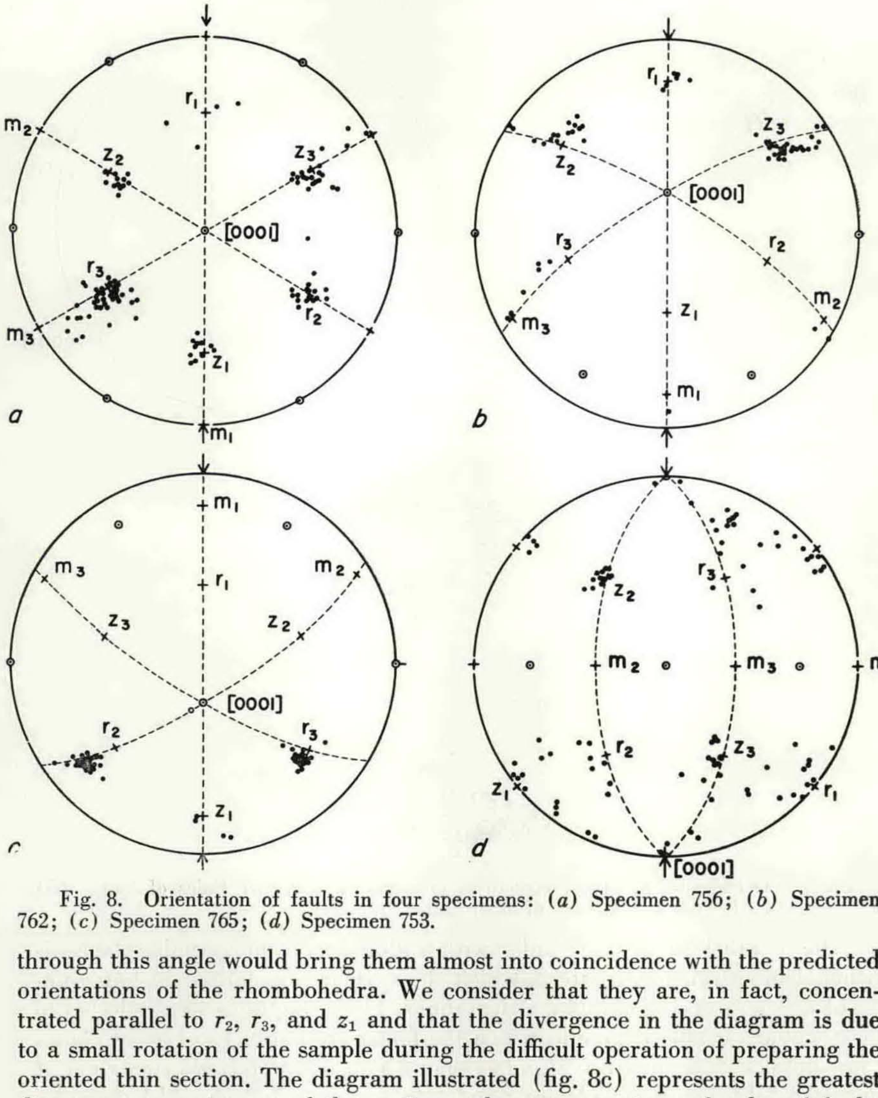

Fig. 8. Orientation of faults in four specimens: (*a*) Specimen 756; (*b*) Specimen 762; (*c*) Specimen 765; (*d*) Specimen 753.

through this angle would bring them almost into coincidence with the predicted orientations of the rhombohedra. We consider that they are, in fact, concentrated parallel to r_2, r_3, and z_1 and that the divergence in the diagram is due to a small rotation of the sample during the difficult operation of preparing the oriented thin section. The diagram illustrated (fig. 8c) represents the greatest divergence seen in any of the sections; the concentrations of poles of faults generally coincided very closely with the predicted orientations of the crystal planes.[3] The greatest spread in the orientation of faults encountered in any of the specimens is illustrated in figure 8d. It is still evident, however, that approximately half of the faults are almost parallel to the unit rhombohedra.

The faults present in all the sectioned specimens are listed in table 2. Where one main set of faults is identifiable it is in bold-face type. The table

[3] The small errors are remarkable in view of the complexity of the methods employed to make the sections. A check on the preservation of the orientation was obtained by optical measurement of the orientation of the *c*-axis and the ends of the cylinders. The departures from the intended orientation were generally less than 5°.

shows the remarkable consistency with which the same crystallographic planes control the faults in cylinders of the same orientation. The most prominent faults are invariably parallel to the basal plane or the unit rhombohedra *r* and *z*. Faults are present in a few specimens more or less parallel to the first order prism *m* and the second order prism *a*, but these are very rare.

The main faults are invariably parallel to planes of high shear stress. Generally when the basal plane or a unit rhombohedral plane is inclined at slightly less than 45° to the axis of loading, the main faults are parallel to this plane. But when the basal or rhombohedral plane with highest shear stress is inclined at slightly more than 45° to the maximum principal stress axis, faulting still takes place parallel to this plane. For example, in C and D cylinders, faulting takes place on rhombohedral planes inclined at approximately 48° to the maximum principal stress axis; in cylinders $\perp m$, the main faults are also rhombohedral planes, inclined at approximately 52° to the axis of compression.

Microtextures in the Deformed Quartz.—The deformed quartz in the samples contains small birefringent haloes (rosettes) which are visible when the sections are close to the extinction positions between crossed polarizers. They are most obvious when the crystal is at extinction as in other positions they are obscured by the higher interference colors of the remainder of the crystal. They appear to be of two distinct sizes: the rays of the larger rosettes range from 0.05 to 0.1 mm in length when the crystals are at extinction; the smaller ones are an order of magnitude smaller than this. Both types are situated in areas of the crystal that are free from faulting or severe fracturing, but the distribution of the two types is different.

Most of the large haloes are associated with the extension fractures parallel to the ends of the cylinders and are located at the inner ends of fractures which extend only part of the way across the crystal (plate 3A, B). A few are isolated and not apparently associated with visible cracks (pl. 3C). A number of the extension cracks in the thin sections do not extend to either side of the crystal, and there is a birefringent halo at each end of these cracks. One further relationship between the haloes and fractures appears to be significant: some of the larger haloes are located on a short fracture in a shear orientation, perfectly parallel to the main faults in the samples; these fractures (approximately 0.1 mm long) change orientation abruptly and become parallel to the ends of the sample; these cracks extend only to one side of the crystal (pl. 3C). The disposition of the bright and dark rays of the rosette-like haloes varies with the crystallographic orientation of the sample and with rotation of the section between crossed polarizers. The structures are most clearly visible in crystals sectioned parallel to the base (1-cut of $\perp$ m cylinders), which are almost isotropic. A few of these large haloes are present in the samples which were unloaded before rupture took place.

The smaller haloes are not associated with cracks and are much commoner than the large. They are much more evenly distributed through the sections and are generally, if not invariably, centered on minute dark inclusions. The bright rays in all the haloes are parallel, giving the quartz a striated appearance in thin section on a fine scale. A close examination of thin sections of the undeformed starting material revealed that a similar texture is present, in less

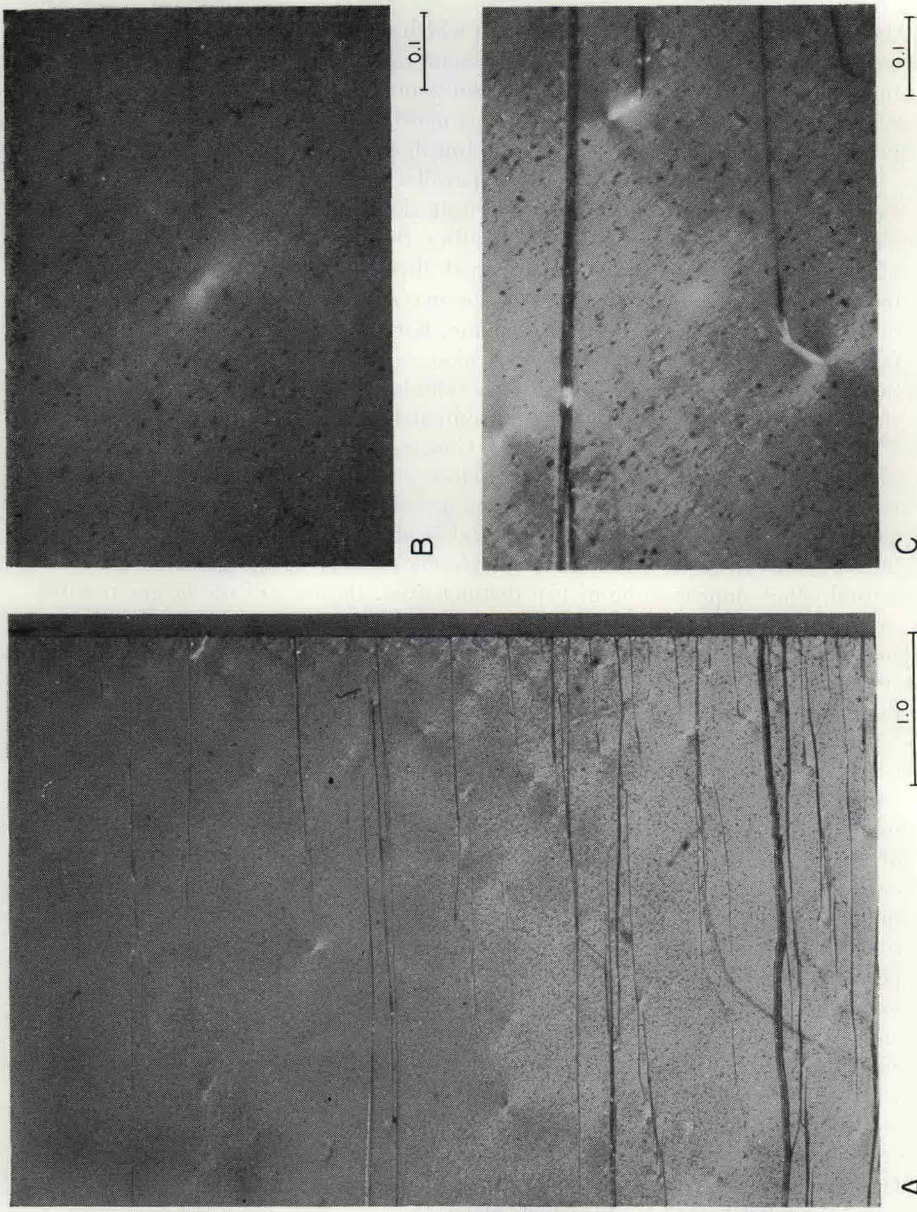

PLATE 3

Photomicrographs between crossed polarizers showing birefringent haloes (rosettes) in deformed samples. Scales are in mm.

A. Portion of sample 756, showing the relationship of haloes to extension fractures. Cylinder axis is north-south. Note localization of haloes at the ends of fractures and, near the center of the photograph, a short fracture terminating in a halo at both ends.

B. A large halo at the end of an extension fracture. Small haloes are also visible in the quartz.

C. Two haloes associated with short shear-fractures, which are deflected and become extension fractures. An isolated halo, unassociated with fractures is visible in the top left, above the extension fracture which traverses the photograph.

marked degree, in the quartz crystals before deformation. Thus the structures, cracks or inclusions, which give rise to this effect are present before deformation, but it is emphasized by the deformation. This effect is visible only in some natural quartz and it has been noted that it is quite common in, and perhaps restricted to, the quartz in igneous rocks (C. Durrell, personal communication).

The haloes must be due either to local rotation of the lattice by plastic deformation or induced birefringence due to residual stresses in the quartz, or a combination of the two effects. The significance of the structures is discussed below.

Other phases in the deformed quartz.—The isotropic material along many of the faults is brownish in plane-polarized light. The zone of isotropic material is extremely thin or absent along some faults, is commonly between 1 and 5 microns thick, and in a few cases is irregular and as thick as 100 microns. Where the zones are thicker than 5 microns, approximately, they contain high proportions of crushed and disoriented quartz fragments. The isotropic material has a refractive index markedly less than the lower index (ω) of quartz. In one of the fault-zones in a section of one deformed crystal there is an aggregate of finely crystalline material (pl. 2D) with low birefringence and refractive indices considerably higher than the higher index (ε) of quartz.

The thinness of the zones of isotropic material and the high proportion of quartz inclusions in them, make it impossible to isolate the material in sufficient quantity for satisfactory optical examination. The material along faults in three samples (separately treated) was removed by scraping with a knife-blade, finely ground in a mortar, and examined in immersion oils. The powdered material was found to consist predominantly of quartz, with only small proportions of other materials. Oils with indices of 1.544 and 1.553 were used with each of the preparations. Of the small amount of isotropic material, most of the grains had a refractive index considerably lower than 1.544, a few between 1.544 and 1.553, and an even smaller number greater than 1.553. In the preparations from two of the samples a few grains were slightly birefringent, with indices considerably higher than 1.553. In order to compare the refractive index of the isotropic material with that of natural silica glass (lechatelierite) the powders were immersed in an oil of index 1.46. All the material appears to have a refractive index greater than 1.46.

The isotropic material seems to have a variable refractive index, though no attempt was made to bracket the values more closely. Most of the material has an index between 1.46 and 1.54. The grains that appeared to have an index above 1.544 may in fact have been cryptocrystalline aggregates of quartz or cryptocrystalline mixtures of quartz and the anisotropic material with high indices, noted above.

The anisotropic material with high indices (>1.553) and low birefringence is probably the same as that identified in the thin section (pl. 2D). It was present in such minute proportions in the powdered samples that no attempt was made to determine the indices in immersion liquids. The relief of the material, by comparison with quartz, is quite marked, however, and the only known phase of silica which has the requisite optical properties is coesite.

DISCUSSION OF DATA

Values of strength.—The values obtained for the strength of quartz in the experiments (table 1) show more internal consistency than those of previous investigators. The strengths determined in the present study are compared with those obtained in experiments at room temperature and various confining pressures by earlier workers in figure 9.

The strengths of cylinders compressed parallel to the *c*-axis (fig. 9a) are similar to those obtained by Bridgman (1941) at confining pressures between 20 and 25 kb in an apparatus using isopentane as the confining medium; but they are considerably lower than those recorded by Griggs and Bell (1938), Bridgman (1940), and Goranson (1949) under similar conditions (fig. 9a). In these experiments Griggs and Bell and Bridgman used lead as the confining medium, and the confining pressure was obtained by a controlled flow of the lead around the piston. Goranson employed a hydrocarbon, which was supposed to retain its low viscosity at high pressures. Griggs, Turner, and Heard (1960, p. 67-68) have discussed these apparently anomalous results and concluded that the results at high pressure in experiments using the lead apparatus may be subject to question; the similarity of Goranson's results to these, however, still represents a problem. Strengths determined at atmospheric pressure by Berndt

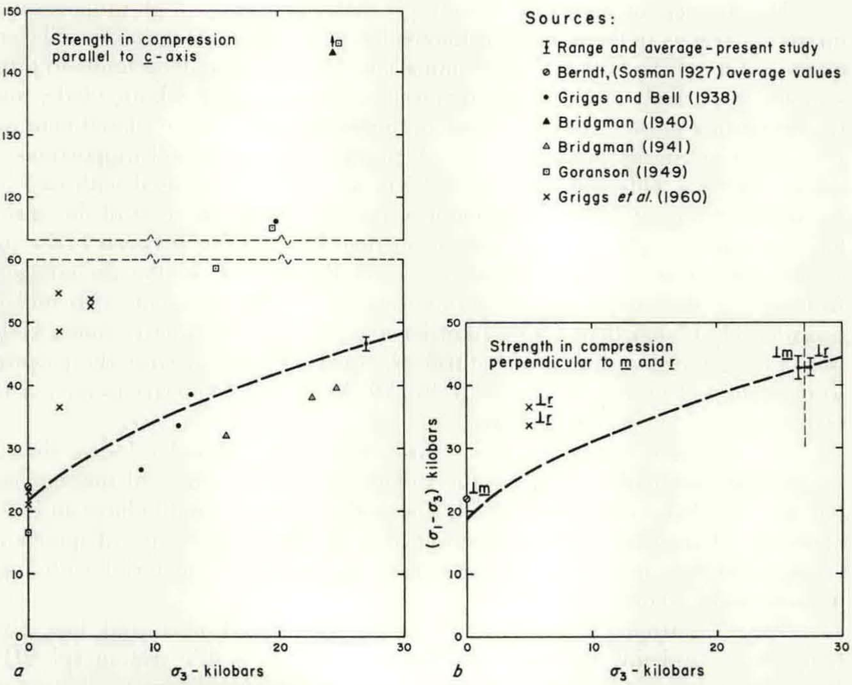

Fig. 9. Strengths of quartz at room temperature and various confining pressures, obtained in the present study and previous studies (as indicated). The broken curves represent strengths predicted by the Griffith theory, using constants derived from the average strengths in the present study.

(*in* Sosman, 1927), Goranson (1949), and Griggs, Turner, and Heard (1960) show a high degree of consistency, but values obtained at confining pressures between one atmosphere and 20 kb are quite variable.

The only previous data available on the strengths at room temperature for other orientations are determinations for compression perpendicular to the *c*-axis at atmospheric pressure (Berndt, in Sosman, 1927) and compression normal to *r* at 5 kb confining pressure (Griggs, Turner, and Heard, 1960). These are represented, with the data from the present study, in figure 9b.

The abnormally high values of strength at high confining pressures obtained by Griggs and Bell (1938), Bridgman (1940), and Goranson (1949) may have been due to high friction at piston-cylinder contacts in their apparatus or to high strength of the confining media employed (Griggs, Turner, and Heard, 1960). Errors due to such effects could not be corrected in the data of these investigators, but should be compensated for in our data as a result of the method of reduction (comparison with a calibration sample of very low shear strength). The values obtained in the present study may be slightly low since no correction was made for the low but finite strength of the indium in the calibration sample.

The origin of the fractures.—The prominent set of planar fractures normal to the cylinder axis is present in samples of all orientations. These fractures are planes of zero shear stress during the experiment; they are also normal to the axis of maximum principal stress during the loading of the sample and obviously could not have developed as extension fractures during loading. The simplest explanation of these features is that they are extension cracks which formed during the unloading of the sample. The fractures appear to be due to stress set up between the copper jacket and the quartz during unloading, for in experiments conducted under similar conditions with soft material, such as silver chloride around the quartz, cracks of this type are not formed.

Similar doubts exist as to the exact time that the other planar and curved fractures (excluding feather-fractures) were produced. It is unlikely that such extension fractures would form at the high pressures that existed in the sample during most of the experiment. They probably formed at the end of the unloading of the sample or even during preparation of the thin sections. It should be noted that they show a rather weak tendency to parallelism with the unit rhombohedra, similar to that demonstrated by Bloss (1957) for fractures produced by grinding at room temperature and pressure, and by Borg and others (1960) for fractures produced in deformation experiments on sand at moderate confining pressures.

The feather-fractures, on the other hand, probably originated along with, or immediately after, the failure of the specimens along the faults. They appear to be extension fractures related to the faults. The fact that these fractures are not quite parallel to the cylinder axis, which is the axis of maximum principal stress in the samples until failure, may reflect the influence of the anisotropy of the crystals, since they show some tendency to be parallel to the unit rhombohedra; but it is equally likely that this reflects the inhomogeneity of the stress after failure, and the feather-fractures may have formed normal to the axis of least principal stress after failure in the vicinity of the faults where they occur.

The nature and origin of the faults.—The nature of the faults is of particular interest because of (a) their parallelism with crystallographic planes and (b) their inclination, in some instances, at angles greater than 45° to the axis of maximum principal stress. There are few data in the literature on the crystallographic orientation of fractures in brittle materials deformed in compression. There are cases reported in which fractures in quartz (Griggs and Bell, 1938) and dolomite (Higgs and Handin, 1959) are non-crystallographic, but in others, such as the quartz crystal illustrated by Griggs and Handin (1960) the fractures are crystallographically controlled. There appears to be no consistency.

The development of faults at angles greater than 45° to the compression axis implies either (1) that if the faults are due entirely to fracture the planes have markedly lower shear strengths than others in the quartz, or (2) that the faulting is due to slip on the planes, since slip is independent of the normal stress on the slip-plane and may therefore occur on planes inclined at angles greater than 45° to the axis of maximum principal stress. The question arises whether the faulting is purely a fracture phenomenon or is initiated by plastic deformation (slip).

That the visible faults are predominantly fracture phenomana is demonstrated by the following features:

(a) There is considerable fracturing on a fine scale in the vicinity of the faults.

(b) The layer of isotropic material along many of the faults forms a discontinuity in the crystal, and the continuity of a crystal is not impaired by slip.

(c) It was not possible to determine the direction of displacement on faults accurately, but in all cases it appeared to be parallel to the direction of maximum resolved shear stress in the fault. For rhombohedral faults, this means that the shear was not parallel to a unique crystal direction, as is generally true of slip.

(d) The sudden shock accompanying failure is characteristic of fracture. It is possible, however, that failure was preceded by slip parallel to the planes of the faults.

It is possible to determine the relative ease with which faulting takes place parallel to different crystal planes (c, r, z, m, a) by comparing (1) the stresses on all possible fault planes in cylinders of a single orientation, at the time of failure (and noting which is the main fault); and (2) the rupture strengths of cylinders of different orientations, in which different crystal planes are expressed as the main faults. Thus in cylinders compressed perpendicular to r_1 and z_1, the shear stress is greater on the other unit rhombohedra (z_2, z_3 and r_2, r_3 respectively) than on the base (c), which is invariably the main fault. It follows that faulting takes place more easily, that is, at lower shear stress, on the base than on the unit rhombohedra. This conclusion is supported by the strength measurements, for cylinders $\perp r$ and $\perp z$, which fault on the base, are consistently weaker than cylinders $\| c$, which fault on the unit rhombohedra, though the main faults in all three types of cylinders are inclined at the same angle (38°) to the axis of compression.

In cylinders compressed perpendicular to m, there is high shear stress on m_2 and m_3 compared with the rhombohedra r_2, r_3 and z_2, z_3, but the main faults are invariably parallel to the rhombohedral planes. Thus faulting appears to take place with greater facility on r and z than m. Similar considerations suggest that shear stresses high enough to cause faulting on the second order prism planes (a) are seldom attained. These conclusions are supported, in a more general way, by the fact that the m and a planes are never present as the main faults, though they are suitably oriented in several types of cylinders.

The evidence clearly indicates that the critical shear stress required for faulting on the basal plane (c) is less than for faulting on the r and z planes; and the shear stress for faulting on r and z is considerably less than for the prisms m and a (table 2).

It is of interest to compare the relative ease of faulting on various crystal planes, as determined above, with the ease of cleavability on these planes. Shappell (1936) and Fairbairn (1939) have calculated the ease of cleavability of quartz parallel to planes of low indices, using the criterion that cleavage will tend to occur along planes that cut the minimum number of bonds per unit area; Fairbairn considered the α-quartz structure and Shappell that of β-quartz. In decreasing tendency to cleave, Shappell lists the planes in the order r and z, a, c, m; Fairbairn lists them in the order r and z, m, c, a. Observations of natural cleavage in quartz (Fairbairn, 1939) support these inferences in that the commonest and most perfect cleavages are invariably parallel to the unit rhombohedra. Cleavage fractures are essentially extension fractures, and both investigators, in deriving their results, considered a tensile stress acting normal to the planes. The density of bonds in the planes might also be expected to influence fracture in response to shear stress on the planes, but it is evident that such considerations do not predict the ease of faulting on these planes, since the shear stress necessary to produce faulting on the base (c) is less than that for faulting on r and z.

It is possible to estimate the theoretical shear strength ("molecular cohesion") of crystals from considerations of the stress required to move an atom in any row into the next similar site in the lattice (Cottrell, 1953). According to the original calculation and assumptions of Frenkel, the critical shear stress necessary to produce such a displacement in a perfect crystal (τ_m) should be $\tau_m = \frac{b}{a} \cdot \frac{\mu}{2\pi}$, where a is the spacing between the planes along which displacements occur, b is the distance between similar atomic sites in the direction of displacement, and μ is the shear modulus in the direction of displacement. Since $a \cong b$ in most crystals $\tau_m \cong \frac{\mu}{2\pi}$. Subsequent refinements of this calculation indicate that the theoretical shear strength of most crystals may be as low as $\frac{\mu}{30}$ (Cottrell, 1953, p. 9).

In the majority of crystalline materials plastic deformation occurs at stresses several orders of magnitude lower than the theoretical strength, but it is well known that quartz and other brittle materials, deformed in compression, may support stresses much closer to the theoretical strength before rupture or plastic flow occurs. The shear moduli in quartz are a few hundred kilobars, and the theoretical shear strengths are therefore an order of magnitude less than this. In compression experiments on quartz at room temperature and pressure, the maximum shear stress in the samples at rupture is approximately 10 kb. At the high confining pressure of the present series of experiments, the shear stress on the main faults at rupture is over 20 kb. The measured shear stresses are therefore within the range of the estimated theoretical values. In view of this, it is of interest to determine whether the shear stress necessary to produce faulting on the various planes varies in the same way as the shear moduli or the theoretical strengths for these planes, calculated according to the above equations.

The shear moduli for certain directions in the planes *c*, *r*, *z*, *m*, and *a* are given in table 3. The values in the table are components C_{ijij} of the elastic stiffness tensor $[C_{ijkl}]$, relating the shear stress (σ_{ij}) in the direction of increasing X_i on the plane perpendicular to the coordinate axis X_j, to the shear strain in the same direction on the same plane (ε_{ij}). The elastic stiffness constants (C_{ijkl}) were calculated from values of the compliance constants (S_{ijkl}) given by Nye (1957, p. 148). The moduli in the required directions were determined by transformation (in cases where this was necessary) according to the standard law for a fourth-rank tensor: $C_{ijij} = a_{im}a_{jn}a_{io}a_{jp}C_{mnop}$. The transformations were carried out with a Bendix G15 computer.

The significance of these values for the problem under consideration is open to doubt, for the following reasons: (1) The elastic constants used in the calculations were determined at low pressure, and the behavior may not be linear up to the high pressures in the experiments; (2) the simple model from which the expression for theoretical strength is derived is a reasonable one for metal structures, but its relevance for a complex framework structure like that of quartz is doubtful. It is clear, in any case, that the relative ease of faulting on the planes *c*, *r*, *z*, *m*, and *a* is not related either to the shear moduli or the theoretical strengths, as calculated above.

TABLE 3

Shear moduli and theoretical strengths for various planes and directions

Plane	Direction	Shear modulus C_{ijij} (kb)	$\frac{b}{a}$	$\frac{C_{ijij}}{2\pi}$	$\left(\frac{b}{a} \cdot \frac{C_{ijij}}{2\pi}\right)$	$\frac{C_{ijij}}{30}$
c {0001}	<01†0> ($\perp m$)	571	1.58	90.9	143.6	19.0
	<10†0> ($\parallel a$)	571	0.91	90.9	82.7	19.0
r $\{10\bar{1}1\}$	<10†1>	384	4.07	61.1	248.7	12.8
z $\{01\bar{1}1\}$	<01†1>	461	4.07	73.4	298.7	15.4
m $\{10\bar{1}0\}$	[0001]	571	1.29	90.9	117.3	19.0
	<10†0>	398	1.15	63.4	72.9	13.3
a $\{11\bar{2}0\}$	[0001]	571	2.20	90.9	200.0	19.0
	<01†0>	398	3.47	63.4	220.0	13.3

The classical theory of brittle fracture, the Griffith theory (Griffith, 1921, 1925), was originally developed to account for the discrepancy between the theoretical and observed strengths of materials. Griffith postulated that solids contain many small cracks, which he represented, in his two-dimensional model, by extremely eccentric elliptical holes. He demonstrated that the stress near the ends of certain holes, of critical length and orientation, may reach the theoretical value when the stress in the material as a whole is considerably below this value. These cracks will then be propagated and lead to failure of the material. Griffith (1925) derived a fracture condition for biaxial states of stress, assuming a mechanically isotropic material containing elliptical cracks of random orientation, the maximum crack-lengths and radii of curvature of the ends of cracks being the same for cracks of all orientations. Failure is predicted when the highest tensile stress at the ends of the longest crack of the most dangerous orientation reaches the value of the theoretical strength of the material. In compression tests the cracks that will propagate and lead to failure are inclined at 45° to the greatest and least principal (compressive) stresses, σ_1 and σ_3 respectively. Fracture should occur when

(1) $\sigma_3 = -K$, if $\sigma_1 + 3\,\sigma_3 < 0$, and

(2) $(\sigma_1 - \sigma_3)^2 - 8K\,(\sigma_1 + \sigma_3) = 0$, if $\sigma_1 + 3\,\sigma_3 > 0$.

The constant K in these equations represents the tensile strength for a uniaxial tensile stress ($\sigma_3 < 0, \sigma_1 = 0$). It has been suggested (Orowan, 1949) that the condition represented by equations (1) and (2) will hold for cases where the stress is triaxial, since normal and shear stresses acting normal to the plane of σ_1 and σ_3 cannot appreciably affect the stresses in this plane. Orowan (1949, p. 201) has shown that the fracture strengths of some brittle materials at high confining pressures can be correlated satisfactorily with their tensile strengths, experimentally determined, using the Griffith fracture criterion. Although the assumptions of mechanical isotropy and, perhaps, random orientation of cracks are not strictly valid for quartz, it is of interest to determine whether the Griffith fracture condition gives a good correlation between the strengths obtained in the present series of experiments and those determined under other conditions.

Since the average strength of crystals compressed parallel to the *c*-axis at 27 kb confining pressure is 46.5 kb, σ_1 and σ_3 at failure are 73.5 kb and 27 kb, respectively. Substituting these values in equation (2) above, a value of the constant K, equal to 2.69 kb, is obtained. This should be the tensile strength of a crystal extended parallel to the *c*-axis. The maximum tensile strength at one atmosphere pressure recorded by Berndt (Sosman, 1927) in thirteen tests was 1.19 kb and the average was 1.1 kb, which are approximately half the value of K. In view of the nature of these tests and the methods by which samples are generally prepared, (by sawing, grinding, or core drilling) the likelihood of surface flaws is high, and measured strengths are likely to be low. Using the value of K obtained above, the strengths ($\sigma_1 - \sigma_3$) at different confining pressures (σ_3) were calculated using the Griffith equation (2). These are represented by the curve in figure 9a. The strengths recorded by Berndt, Goranson (1949) and Griggs, Turner, and Heard (1960), at one bar confining pressure, Griggs and Bell (1938) at 8 to 15 kb, and Bridgman (1941) at 15 to 25 kb lie quite close to this curve. On the other hand, values of strength obtained by Griggs, Turner, and Heard (1960) at 2.5 to 5 kb and some of those obtained by Bridgman (1940), Goranson (1949), and Griggs and Bell (1938) at higher confining pressures are considerably higher than the strengths indicated by the curve (fig. 9a). For reasons noted above, these latter measurements may be higher than the true values.

The experimental data for cylinders compressed perpendicular to r and m are represented in figure 9b, along with the curve of the Griffith equation, calculated using values of K obtained from our strength determinations. The two values of K are almost identical (K is 2.35 and 2.36 kb for r and m cylinders, respectively), and the values of $(\sigma_1 - \sigma_3)$ for both orientations are represented by a single curve. Few data are available on the strength for these orientations at other confining pressures.

No definite conclusions can be drawn as to the consistency of the data with the predictions of the Griffith theory of brittle fracture. But many of the earlier strength measurements, particularly those made in compression tests at one atmosphere, which are not likely to involve such large errors as measurements at high confining pressures, can be satisfactorily correlated with the measurements made in the present study by means of the Griffith fracture criterion.

It was demonstrated above that faulting takes place at lower shear stress on the base than on r and z and on r and z than on m and a. It was shown that this is not accounted for by the bond density across these planes, as in cleavage development, or ~~to~~ by the elastic moduli. Nor is it in accord with the theoretical strengths for slip in these planes in the direction of the shear displacements on the faults. This is not unusual, as the plasticity of crystals is not generally related to their behavior below the elastic limit. To determine if the shear strengths along these planes are limited by plastic yielding, we should therefore consider the actual plastic behavior of quartz, insofar as this is known. Large plastic deformations of quartzite and quartz single crystals were recently obtained for the first time in the laboratory of D. T. Griggs (Carter, Christie, and Griggs, 1961; Christie, Carter, and Griggs, in press). In short tests quartz flows plastically at high confining pressures (above 15 kb) and moderate to high temperatures (300° to 1500°C) and also at lower pressure (5 kb) and moderate temperatures (300° to 500°C) in tests at slow strain-rates (Heard, 1962). Under these conditions slip on the base (c) is the commonest mechanism, but other mechanisms also operate; there is evidence that the other slip-planes include the rhombohedra r and z, and possibly also the prism planes. The critical resolved shear stress for basal slip is lower than for the other mechanisms. It is therefore possible to account for the greater ease of faulting on the base than on the other planes if it is postulated that faulting in our experiments is initiated by small amounts of slip on the planes.

The hypothesis that the faulting is initiated by small amounts of plastic flow is not inconsistent with the use of the term "brittle fracture" for the phenomenon. The term "brittle fracture" specifies only the mode of propagation of the existing cracks in a stressed body: it denotes that the only work done in crack propagation is that required to overcome the cohesive forces between atoms on both sides of the crack and this may be derived from the strain energy of the crystal; this distinguishes it from "ductile fracture", in which material must be deformed plastically at the ends of cracks for propagation to take place (Orowan, 1949). The work done in the latter process is much greater than that required to overcome the cohesive forces. The initial flaws or cracks which give rise to either brittle or ductile fracture may be produced by small plastic deformations. However, this hypothesis implies that there need be no relationship between the measured strengths and the curve predicted by the Griffith equation (above) since the factor which controls strength in this hypothesis is the stress necessary to induce the movement of dislocations (plastic flow) which produce the initial cracks, rather than the stress necessary to propagate pre-existing cracks.

In recent years the mechanisms of fracturing in many different materials have been intensively studied (Averbach and others, 1959). It has been shown that plastic deformation commonly precedes brittle fracture and that several dislocation mechanisms may give rise to cracks large enough to be "dangerous" in the Griffith sense and propagate as brittle fractures. In particular, high stress concentrations may develop at the intersections of primary and secondary slip bands, due to the pile-up of dislocations, and give rise to the initial cracks (Cottrell, 1959). This mechanism has been demonstrated in MgO crystals by Parker (1959) and Stokes, Johnston, and Li (1959). Parker considers that most cracks originate in a {100} cleavage plane, which is equally inclined to the two {110} slip-planes at their intersection, though he also reports some cracks originating parallel to the slip-planes. Stokes, Johnston, and Li (1959) have shown that the cracks in their experiments all originate in the {110} slip-planes. The resulting fracture is typically brittle in these experiments. Various other dislocation models have been suggested for initiating cracks, which may subsequently grow as either brittle or ductile fractures (Orowan, 1954; Hahn and others, 1959; Cottrell, 1959).

The most satisfactory hypothesis to explain the crystallographic nature of the faults is that cracks were initiated by yielding and slight plastic flow on certain planes, notably c, r, and z, and then propagated rapidly in these planes by the brittle fracture mechanism.

The Nature of the Microtextures.—The larger birefringent haloes or rosettes are generally, though not invariably, associated with extension fractures parallel to the ends of the cylinders, formed during unloading of the samples. This suggests that they may be due to residual stress at the leading edge of the cracks. To test this, a polished basal plate of quartz, less than 2 mm thick, was fractured so that some cracks extended part way into the crystal; the plate was observed on a polarizing microscope with the analyzer rotated to compensate for the rotation of the plane of polarization in the plate, and a crack was propagated slowly by pressure on the plate. The birefringent halo at the end of the advancing crack was minute compared with the features in our samples, in spite of the greater thickness of the plate. It is therefore clear that the haloes in the samples are not due merely to residual stress at the ends of the extension cracks. This implies the presence of comparatively large permanent strains at the sites of the birefringent features. It is probable also that the transverse extension fractures originated at these sites, where the residual stresses must also be large. The existence of isolated haloes and the termination of some cracks in a halo at each end are consistent with this conclusion.

The birefringent haloes are similar in general character to a birefringent rosette photographed with polarized infrared radiation in silicon by Bond and Andrus (1956). This was attributed to the stress around a single edge dislocation; the rosette is considerably smaller than those in the deformed quartz. Similar features have been observed in corundum and Rochelle Salt crystals and attributed to the stress around "macroscopic edge dislocations" (Indenbom, 1958). Such a macroscopic dislocation would most probably consist of a locked array of actual edge dislocations of similar sign lying in one plane. The stresses due to such an array would be much greater than those around a single dislocation (Koehler, 1952). The association of some of the large haloes in our samples with short fractures parallel to the main faults suggests that the faults may originate at regions similar to those represented by the haloes. Thus the birefringent haloes probably constitute visible evidence of plastic deformation which preceded the fracturing along fault-planes.

The Origin of New Phases.—The isotropic material along the faults in the samples may be glassy material which originated by fusion of the quartz along the faults or it may have been formed by extreme mechanical disruption of the quartz in the immediate vicinity of the shear-planes. In view of the very small displacements on some of the faults the latter alternative is doubtful, and the former will be considered in more detail.

Most of the large samples contain less than 50 faults of area 1 cm^2, and the average thickness of the zones of isotropic material is less than 10 microns; the total volume of isotropic material in these samples is therefore less than 0.05 cm^3. The heat required to raise the temperature of this quartz to the melting point and produce fusion can be calculated approximately. The temperatures of the α-β transition and melting at the high pressures of the experiments are not known, but it is assumed that the transition will occur at approximately 1200°C and melting at 2000°C, consistent with the extrapolated and inferred phase boundaries given by Boyd and England (1960b). From the data given by Goranson (1942) on the heat capacities and heat of fusion of quartz, the heat content at the melting point plus the heat of fusion is approximately 600 cal per gm. These data were determined at one atmosphere, but calculations show that the values of heat content at 30 kb differ by only a few percent from those at one atmosphere. Since the volume of isotropic material in the large samples is 0.05 cm^3 or approximately 0.12 gm, the energy required to heat and melt this material is 72 cal; the mechanical equivalent of this energy is approximately 3×10^9 ergs. This should be compared with the elastic strain energy of the system immediately before rupture of the samples to determine whether actual fusion of the quartz along the faults might have occurred.

The elastic strain energy of the system comprises the strain energy of the crystal and that of the apparatus, including the piston, pressure vessel, hydraulic system, and structural framework. Of these, only the elastic strain energy of the crystal sample can be estimated. The apparatus is very large compared with the crystal, and the strain energy of the apparatus is greater, perhaps by orders of magnitude, than that of the crystal. The elastic strain energy (W) in the samples is given, in matrix notation (Nye, 1957, p. 137), by

$$\begin{aligned} W &= \tfrac{1}{2} C_{ij}\, \varepsilon_i\, \varepsilon_j \\ &= \tfrac{1}{2} \sigma_i\, \varepsilon_i \\ &= \tfrac{1}{2} S_{ij}\, \sigma_i\, \sigma_j \end{aligned}$$

Substituting values of the compliance constants (Nye, 1957, p. 148) and the stress in the samples immediately before rupture, the strain energy density (in cylinders compressed parallel to the *c*-axis and normal to *m*) is found to be approximately 3×10^9 ergs/cm^3. The strain energy in the larger samples (volume 2 cm^3) is therefore of the order of 6×10^9 ergs.

Thus the energy necessary to cause fusion along the faults, to the extent indicated by the isotropic material, is less than the elastic strain energy of the crystal by only a small factor. It should also be remembered that the work done in producing the fractures is also derived from the strain energy of the system. However, inasmuch as the elastic strain energy of the apparatus is much greater than that of the crystal, it appears to be possible that the isotropic material originated by fusion, if the elastic strain energy was rapidly dissipated as heat along the faults, as a result of friction.

It was shown that the refractive index of the isotropic material was variable but invariably greater than that of the common form of silica glass, lechatelierite. This may be due to imperfect destruction of the quartz structure, or the packing of the atoms or Si-O groups may be denser, because of the extremely high pressures of formation, than in lechatelierite.

Although the conditions in the samples at rupture probably are within the stability field of coesite (from a linear extrapolation of the phase boundary determined by Boyd and England, 1960b) coesite was not expected to form in the experiments in view of the sluggishness of the transformation, Quartz $\rightleftarrows$ Coesite, at low temperatures (MacDonald, 1956; Boyd and England, 1960b). MacDonald found that runs made in a simple squeezer at 400°C require almost a day to yield coesite. However, the transformation may have been accelerated locally along the faults by heat derived from the sudden conversion of strain energy at rupture, just as fusion may have taken place in the vicinity of the faults.

Geological Significance.—The conditions in the experiments do not simulate those in the earth's crust under normal conditions: the mean pressures are equivalent to those at depths of about 100 km, and the temperature is that of rocks at the surface; moreover, the stress differences $(\sigma_1 - \sigma_3)$ at rupture are much greater than those which may exist within the crust in normal circumstances. The experiments were originally designed to attempt to produce plastic deformation of quartz and from this viewpoint they demonstrate only that *extensive* plastic deformation does not take place under these conditions.

The experiments may, however, be of direct relevance for studies of quartz-bearing rocks at the sites of meteoritic impact, where the initial deformation is extremely rapid and may take place at low temperatures. Extremely high pressures and differential stresses are also generated on impact. The conditions locally at impact sites may be similar to those in our experiments, and structures like those in our samples may be produced in rocks which are not completely disrupted or heated to high temperatures near the center of impact.

ACKNOWLEDGMENTS

We are indebted to D. T. Griggs for suggesting the experimental method used in the study, for many profitable discussions and constructive criticism of the manuscript; and to G. C. Kennedy for the use of the high-pressure equipment. We wish to thank R. L. Shreve for considerable assistance in preparing a program for computing the transformations of the elastic constants of quartz and for reading the manuscript. W. G. Ernst and G. Oertel also contributed to the study by discussion and criticism of the manuscript. The unusually difficult work of preparing the thin sections was done by J. de Grossé. Mrs. Peter Kurtz drafted the figures and table.

Costs of equipment and portions of the work were covered by Nonr Grant 233(28), N.S.F. Grant G 6541, and Grant 678A of the Petroleum Research Fund of the American Chemical Society.

REFERENCES

Averbach, B. L., Felbeck, D. K., Hahn, G. T., and Thomas, D. A., eds., 1959, Fracture: New York, John Wiley and Sons, 646 p.

Billings, M. P., 1954, Structural Geology (2d ed.): New York, Prentice-Hall, Inc., 514 p.

Bloss, F. D., 1957, Anisotropy of fracture in quartz: Am. Jour. Sci., v. 255, p. 214-225.

Bond, W. L., and Andrus, J., 1956, Photographs of the stress field around edge dislocations: Phys. Rev., v. 101, p. 1211.

Borg, I., Friedman, M., Handin, J., and Higgs, D. V., 1960, Experimental deformation of St. Peter Sand, *in* Griggs, D. T., and Handin, J., eds., Rock Deformation, Geol. Soc. America Mem. 79, p. 133-191.

Boyd, F. R., and England, J. L., 1960a, Apparatus for phase-equilibrium measurements at pressures up to 50 kilobars and temperatures up to 1750°C: Jour. Geophys. Research, v. 65, p. 741-748.

——— 1960b, The quartz-coesite transition: Jour. Geophys. Research, v. 65, p. 749-756.

Bridgman, P. W., 1940, New high pressures reached with multiple apparatus: Phys. Rev., v. 57, p. 342-343.

——— 1941, Explorations toward the limit of utilizable pressures: Jour. Appl. Physics, v. 12, p. 461-469.

Carter, N. L., Christie, J. M., and Griggs, D. T., 1961, Experimentally produced deformation lamellae and other structures in quartz sand [abs.]: Jour. Geophys. Research, v. 66, p. 2518-2519.

——— in press, Experimental deformation and recrystallization of quartz: Jour. Geology, in press.

Christie, J. M., Carter, N. L., and Griggs, D. T., 1961, Experimental evidence for a basal slip mechanism in quartz [abs.]: Science, v. 134, p. 1427.

——— in press, Experimental evidence of basal slip in quartz: Jour. Geology, in press.

Coes, L., Jr., 1955, High pressure minerals, Am. Ceramic Soc. Jour., v. 38, p. 298.

Cottrell, A. H., 1953, Dislocations and plastic flow in crystals: Oxford, Clarendon Press, 223 p.

——— 1959, Theoretical aspects of fracture, *in* Averbach, B. L., Felbeck, D. K., Hahn, G. T., and Thomas, D. A., eds., Fracture: New York, John Wiley and Sons, p. 20-44.

Fairbairn, H. W., 1939, Correlation of quartz deformation with its crystal structure: Am. Mineralogist, v. 24, p. 351-368.

Goranson, R. W., 1942, Handbook of Physical Constants: Geol. Soc. America Spec. Paper 36, sec. 16, p. 223-242.

——— 1949, Effect of pressure on physical phenomena in the crust: Am. Geophys. Union Trans., v. 30, p. 187-189.

Griffith, A. A., 1921, The phenomena of flow and rupture in solids: Royal Soc. [London] Philos. Trans., ser. A, v. 221, p. 163-198.

——— 1925, The theory of rupture: Internat. Cong. Appl. Mech., 1st, Delft 1924, Proc. p, 55-63.

Griggs, D. T., and Bell, J. F., 1938, Experiments bearing on the orientation of quartz in deformed rocks: Geol. Soc. America Bull., v. 49, p. 1723-1746.

Griggs, D. T., and Handin, J., 1960, Observations on fracture and a hypothesis of earthquakes, *in* Griggs and Handin, eds., Rock Deformation: Geol. Soc. America Mem. 79, p. 347-364.

Griggs, D. T., Turner, F. J., and Heard, H. C., 1960, Deformation of rocks at 500° to 800°C., *in* Griggs and Handin, eds., Rock Deformation: Geol. Soc. America Mem. 79, p. 39-104.

Hall, H. T., 1958, Some high pressure, high temperature apparatus design considerations: Rev. Sci. Instruments, v. 29, p. 267-275.

Hahn, G. T., Averbach, B. L., Owen, W. S., and Cohen, M., 1959, Initiation of cleavage microcracks in polycrystalline iron and steel, *in* Averbach, B. L., Felbeck, D. K., Hahn, G. T., and Thomas, D. A., eds., Fracture: New York, John Wiley and Sons, p. 91-114.

Heard, H. C., ms, 1962, The effect of large changes in strain rate in the experimental deformation of rocks: Ph.D. thesis, Univ. of California, Los Angeles.

Higgs, D. V., and Handin, J., 1959, Experimental deformation of dolomite single crystals: Geol. Soc. America Bull., v. 70, p. 245-277.

Ichikawa, Shimmatsu, 1915, Studies on the etched figures of Japanese quartz: Am. Jour. Sci., 4th ser., v. 39, p. 455-473.

Indenbom, V. L., 1958, Dislocations in crystals: Kristallografia, v. 3, p. 112-132 [English translation].

Kennedy, G. C., and LaMori, P. N., 1961, Some fixed points on the high pressure scale, *in* Bundy, Hibbard, and Strong, eds., Progress in Very High Pressure Research, Internat. Conf., Bolton Landing 1960, Proc.: New York, John Wiley and Sons, Inc., p. 304-311.

——— 1962, The pressures of some solid-solid transitions: Jour. Geophys. Research, v. 67, p. 851-856.

Koehler, J. S., 1952, The production of large tensile stresses by dislocations: Phys. Rev., v. 85, p. 480-481.

MacDonald, G. J. F., 1956, Quartz-coesite stability relations at high temperatures and pressures: Am. Jour. Sci., v. 254, p. 713-721.

Nye, J. F., 1957, Physical properties of crystals: Oxford, Clarendon Press, 322 p.

Orowan, E., 1949, Fracture and strength of solids: Phys. Soc. [London], Progress in Physics Repts., v. 12, p. 185-232.

——— 1954, Dislocations and mechanical properties, *in* Cohen, M., ed., Dislocations in Metals: New York, Am. Inst. Mining Metall. Eng., Inc., chap. 3, p. 69-195.

Parker, E. R., 1959, Fracture of ceramic materials, *in* Averbach, B. L., Felbeck, D. K., Hahn, G. T., and Thomas, D. A., eds., Fracture: New York, John Wiley and Sons, p. 181-192.

Shappell, M. D., 1936, Cleavage of ionic minerals: Am. Mineralogist, v. 21, p. 75-102.

Sosman, R. B., 1927, Properties of silica: New York, Chem. Catalog Company, 856 p.

Stokes, R. J., Johnston, T. L., and Li, C. H., 1959, Discussion *in* Averbach, B. L., Felbeck, D. K., Hahn, G. T., and Thomas, D. A., eds., Fracture: New York, John Wiley and Sons, p. 192.